

SPECTRAL REGROWTH ANALYSIS OF BAND-LIMITED OFFSET-QPSK

J. Nsenga^{1,2}, W. Van Thillo^{1,2}, A. Bourdoux², V. Ramon², F. Horlin³, R. Lauwereins^{1,2}

¹ESAT-KUL, Kasteelpark Arenberg 10, B-3001 Leuven, Belgium

²IMEC, Kapeldreef 7, B-3001 Leuven, Belgium

³ULB, Avenue F. D. Roosevelt 50, B-1050 Bruxelles, Belgium

ABSTRACT

In this paper, we present an analytical analysis to predict the Power Spectral Density (PSD) at the output of a nonlinear Power Amplifier (PA). We focus on Offset Quadrature Phase Shift Keying (OQPSK) waveform band-limited by a Square Root Raised Cosine (SRRC) filter. This is one of the waveforms used in Wideband Code Division Multiple Access (W-CDMA) wireless standard. We show that the PA output PSD obtained by our analytical analysis matches well the simulated PSD. Furthermore, we compare the PA output PSD of QPSK and OQPSK waveforms as a function of the SRRC filter roll-off. We conclude that for small roll-off, both QPSK and OQPSK experience almost the same level of spectral regrowth. As the roll-off increases, OQPSK becomes less sensitive to PA nonlinearity relative to QPSK.

Index Terms— Spectral analysis, Correlation, Power amplifier nonlinearities, Offset Quadrature Phase Shift Keying, Interchannel interference .

1. INTRODUCTION

The Power Amplifier (PA) is the main energy consuming component of current wireless communication systems [1]. In order to achieve higher power efficiency, the PA operating point is chosen near (or completely in) the saturation region [2]. However, the operation of a PA in this region distorts the waveform of time-varying envelope signals, which causes higher out-of-band power emissions. This phenomenon is commonly known as Spectral Regrowth (SR) of side lobes.

SR due to nonlinear amplification is observed on the Power Spectral Density (PSD) of the PA output signal. Several studies have been carried out to predict analytically the PA output PSD [3–5]. In [3], a closed-form expression of the PA output PSD is obtained assuming Gaussian input signals. However, the Gaussian assumption is not valid for most communication signals. Later on, Raich and Zhou have presented an analytical study to derive the PA output PSD of real communication signals, with a special focus on Quadrature Phase Shift Keying (QPSK) [4]. In [5], the same authors compare the PA output PSD of both QPSK and Offset QPSK

(OQPSK). Nevertheless, since their analysis considers a half-sine pulse shaping filter, the resulting OQPSK waveform has a constant envelope. Therefore it does not experience any SR at the output of a nonlinear PA. In fact, the analytical analysis presented in both [4, 5] cannot be used to derive analytically the PA output PSD of time-varying envelope OQPSK waveforms.

In current wireless standards like Wideband Code Division Multiple Access (W-CDMA), OQPSK waveforms are band-limited by a Square Root Raised Cosine (SRRC) filter. This filter has better spectral efficiency property than a half-sine filter. However, in this case, the waveform of an SRRC-OQPSK has a time-varying envelope. Thus, it becomes interesting to predict analytically the SR of SRRC-OQPSK waveform at the output of a nonlinear PA.

In this paper, we present an analytical analysis to derive the PA output PSD of band-limited offset type modulated signals (in this paper, OQPSK signals) as a function of PA characteristics and band-limiting filters. Our analysis can also be used to predict the PA output PSD of non-offset type modulation schemes. As a study case, we focus on QPSK and OQPSK modulation schemes since the choice between them is always a difficult task.

The paper is organized as follows. In Section 2, the system model is described. The analytical derivation of the PA output PSD is presented in Section 3. In Section 4, we validate our analytical approach and use it to compare PA output PSD of both QPSK and OQPSK. Finally, our conclusions are drawn in Section 5.

2. SYSTEM MODEL

Let us consider the equivalent low-pass transmitter model represented in Figure 1. The in-phase and the quadrature symbols are respectively denoted i_n and q_n . The transmitted symbols i_n and q_n form two mutually independent random set I and Q . Each set is independent identically distributed (i.i.d) and has a symmetric distribution. Since the communication channel is band-limited to some specified bandwidth W Hz, the symbols i_n and q_n are pulse shaped by filters with impulse responses $g_I(t)$ and $g_Q(t)$ respectively. The specific offset

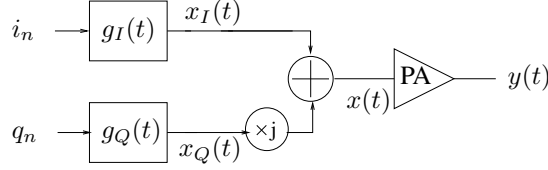


Fig. 1. Equivalent low-pass transmitter model

between the in-phase and quadrature paths (characteristic of OQPSK waveforms) is modeled through the quadrature filter such that $g_Q(t) := g_I(t - T/2)$, with T representing the symbol period. Note that for QPSK waveform, both filters $g_I(t)$ and $g_Q(t)$ are identical. The equivalent low pass signal at the PA input, denoted $x(t)$, is then given by:

$$x(t) = x_I(t) + jx_Q(t), \quad (1)$$

with

$$x_I(t) = \sum_{n=-\infty}^{\infty} i_n g_I(t - nT), \quad (2a)$$

$$x_Q(t) = \sum_{n=-\infty}^{\infty} q_n g_Q(t - nT). \quad (2b)$$

Next, the signal $x(t)$ is amplified by a nonlinear PA. In this study, the PA nonlinearity is described by a memoryless polynomial model from [6]. The equivalent low-pass signal at the PA output, denoted $y(t)$, is given by:

$$y(t) = x(t) \sum_{k=0}^K a_{2k+1} |x(t)|^{2k}, \quad (3)$$

where coefficients a_{2k+1} are complex-valued. In the following, we limit our analysis to nonlinearity of 3rd order ($K = 1$). However, our approach can be straightforwardly extended to higher order nonlinearities.

3. DERIVATION OF THE PA OUTPUT PSD

The PSD of a stationary random signal is obtained by taking the Fourier transform of its autocorrelation function [7]. However, considering the system model described in Section 2, the symbols i_n and q_n are transmitted at discrete time instants so that the resulting signals $x(t)$ and $y(t)$ are not stationary. In order to ensure their stationarity, we introduce in (1) a random time shift T_0 that is uniformly distributed between $[0, T]$. Therefore, the PA input signal becomes:

$$\hat{x}(t) := x(t - T_0). \quad (4)$$

The stationary signal $\hat{x}(t)$ yields at the PA output a stationary signal $\hat{y}(t)$. The autocorrelation function of $\hat{y}(t)$ is given by:

$$R_{\hat{y}}(\tau) = E[\hat{y}(t)\hat{y}^*(t + \tau)], \quad (5)$$

where E and $*$ represent the expectation and the conjugate operators respectively. Replacing the stationarized expression of (3) in (5), we get:

$$\begin{aligned} R_y(\tau) &= |a_1|^2 \underbrace{E[\hat{x}(t)\hat{x}^*(t + \tau)]}_{R_{11}(\tau)} \\ &+ a_1 a_3^* \underbrace{E[|\hat{x}(t)|^2 \hat{x}(t) \hat{x}^*(t + \tau)]}_{R_{31}(\tau)} \\ &+ a_3 a_1^* \underbrace{E[\hat{x}^*(t + \tau) |\hat{x}(t)|^2 \hat{x}(t)]}_{R_{31}(\tau)} \\ &+ |a_3|^2 \underbrace{E[|\hat{x}(t)|^2 \hat{x}(t) |\hat{x}(t + \tau)|^2 \hat{x}^*(t + \tau)]}_{R_{33}(\tau)} \end{aligned} \quad (6)$$

Next, taking into account on the one hand the uncorrelatedness (conditioned on T_0) between $\hat{x}_I(t)$ and $\hat{x}_Q(t)$ and on the other hand the zero-mean properties of both $\hat{x}_I(t)$ and $\hat{x}_Q(t)$ (by symmetry), we obtain from (6):

$$R_{11}(\tau) = E[\hat{x}_I(t)\hat{x}_I(t + \tau)] + E[\hat{x}_Q(t)\hat{x}_Q(t + \tau)] \quad (7a)$$

$$\begin{aligned} R_{13}(\tau) &= E[\hat{x}_I(t)\hat{x}_I^3(t + \tau)] + E[\hat{x}_Q(t)\hat{x}_Q^3(t + \tau)] \\ &+ E[\hat{x}_I(t)\hat{x}_Q^2(t + \tau)\hat{x}_I(t + \tau)] \\ &+ E[\hat{x}_Q(t)\hat{x}_I^2(t + \tau)\hat{x}_Q(t + \tau)] \end{aligned} \quad (7b)$$

$$\begin{aligned} R_{31}(\tau) &= E[\hat{x}_I^3(t)\hat{x}_I(t + \tau)] + E[\hat{x}_Q^3(t)\hat{x}_Q(t + \tau)] \\ &+ E[\hat{x}_I^2(t)\hat{x}_Q(t)\hat{x}_Q(t + \tau)] \\ &+ E[\hat{x}_Q^2(t)\hat{x}_I(t)\hat{x}_I(t + \tau)] \end{aligned} \quad (7c)$$

$$\begin{aligned} R_{33}(\tau) &= E[\hat{x}_I^3(t)\hat{x}_I^3(t + \tau)] + E[\hat{x}_Q^3(t)\hat{x}_Q^3(t + \tau)] \\ &+ E[\hat{x}_I^3(t)\hat{x}_Q^2(t)\hat{x}_I(t + \tau)] \\ &+ E[\hat{x}_Q^3(t)\hat{x}_I^2(t)\hat{x}_Q(t + \tau)] \\ &+ E[\hat{x}_I^2(t)\hat{x}_Q(t)\hat{x}_I^2(t + \tau)\hat{x}_Q(t + \tau)] \\ &+ E[\hat{x}_Q^2(t)\hat{x}_I(t)\hat{x}_Q^2(t + \tau)\hat{x}_I(t + \tau)] \\ &+ E[\hat{x}_I^2(t)\hat{x}_Q(t)\hat{x}_Q^3(t + \tau)] \\ &+ E[\hat{x}_Q^2(t)\hat{x}_I(t)\hat{x}_I^3(t + \tau)]. \end{aligned} \quad (7d)$$

Note that $\hat{x}_I(t)$ and $\hat{x}_Q(t)$ are real-valued signals, thus we may omit the conjugate operator on the second terms in the

expectations. A general expression of the above different expectations is:

$$E^{(U,V,M,N)} = E[\hat{x}_I^U(t)\hat{x}_I^V(t+\tau)\hat{x}_Q^M(t)\hat{x}_Q^N(t+\tau)], \quad (8)$$

where $(U + V)$ and $(M + N)$ are even and belong to the set $\{0, 2, 4, 6\}$ for the 3^{rd} order nonlinearity. Afterwards, we substitute in (8) the signals $\hat{x}_I(t)$ and $\hat{x}_Q(t)$ by respectively stationarized expressions (2a) and (2b). Then, exploiting the mutual independence between i_n , q_n and T_0 random variables, we get:

$$\begin{aligned} E^{(U,V,M,N)} = & \sum_{n_1} \dots \sum_{n_U} \sum_{n_{U+1}} \dots \sum_{n_{U+V}} \sum_{m_1} \dots \sum_{m_M} \sum_{m_{M+1}} \dots \sum_{m_{M+N}} \\ & \times E[i_{n_1} \dots i_{n_U} i_{n_{U+1}} \dots i_{n_{U+V}}] \quad (9a) \\ & \times E[q_{m_1} \dots q_{m_M} q_{m_{M+1}} \dots q_{m_{M+N}}] \quad (9b) \\ & \times E\left[\prod_{i=1}^U g_I(t - n_i T - T_0) \prod_{i=U+1}^{U+V} g_I(t + \tau - n_i T - T_0) \right. \\ & \left. \prod_{q=1}^M g_Q(t - m_q T - T_0) \prod_{q=M+1}^{M+N} g_Q(t + \tau - m_q T - T_0)\right]. \quad (9c) \end{aligned}$$

The summation indices n_l and m_k (with $l = 1, \dots, U + V$ and $k = 1, \dots, M + N$) represent respectively different transmission instants of i_{n_l} and q_{m_k} symbols. Each of them varies from $-\infty$ to ∞ .

In the following, we describe how the different factors (9a), (9b) and (9c) are further developed.

Firstly, we use cumulants operators to evaluate higher order statistics in (9a) and (9b) [8]. Let X represents the set I or Q . The k^{th} cumulant-to-moment conversion formula is defined as [8]:

$$E[x_{n_1} x_{n_2} \dots x_{n_k}] = \sum_{U_{p=1}^z X_p = X} \prod_{p=1}^z \text{cum}(X_p), \quad (10)$$

where the summation extends over all partitions of set X , meaning the unordered collection of non-intersecting non-empty sets X_p such that $\bigcup_{p=1}^z X_p = X$ (cfr [8]). The notation U represents the union operator while the variable z denotes the number of non-empty sets in one given partition of set X .

$$\begin{aligned} E^{(2,2,1,1)} = & \frac{\gamma_{4,I}\gamma_{2,Q}}{T} \sum_n \int_{-\infty}^{\infty} g_I^2(t)g_I^2(t+\tau)g_Q(t-nT)g_Q(t+\tau-nT)dt \\ & + \frac{\gamma_{2,I}^2\gamma_{2,Q}}{T} \sum_{n_1} \sum_{n_2} \int_{-\infty}^{\infty} g_I^2(t)g_I^2(t+\tau-n_1T)g_Q(t-n_2T)g_Q(t+\tau-n_2T)dt \\ & + 2\frac{\gamma_{2,I}^2\gamma_{2,Q}}{T} \sum_{n_1} \sum_{n_2} \int_{-\infty}^{\infty} g_I(t)g_I(t+\tau)g_I(t-n_1T)g_I(t+\tau-n_1T)g_Q(t-n_2T)g_Q(t+\tau-n_2T)dt \quad (13) \end{aligned}$$

Since I and Q have the i.i.d property, their k^{th} -order cumulant are multidimensional Dirac functions [8]. They can be written as:

$$\text{cum}(x_{n_1}, x_{n_2}, \dots, x_{n_k}) = \gamma_{k,x} \prod_{l=2}^k \delta(n_1 - n_l), \quad (11)$$

with $\gamma_{k,x}$ is the k^{th} order cumulant at lag 0. For instance, $\gamma_{2,x}$ and $\gamma_{4,x}$ represent respectively the variance and kurtosis of x .

Secondly, in the factor (9c), by taking into account that the random variable T_0 is uniformly distributed over the interval $[0, T]$, we obtain:

$$\begin{aligned} & \frac{1}{T} \int_0^T \prod_{i=1}^U g_I(t - n_i T - T_0) \prod_{i=U+1}^{U+V} g_I(t + \tau - n_i T - T_0) \\ & \prod_{q=1}^M g_Q(t - m_q T - T_0) \prod_{q=M+1}^{M+N} g_Q(t + \tau - m_q T - T_0) dT_0. \quad (12) \end{aligned}$$

At this point, we have all the necessary tools to derive the analytical expression of each particular expectation described by (8). As an example, for $U = 2, V = 2, M = 1$ and $N = 1$, after mathematical manipulations we end up with the expression given in (13). The high order cross-correlation between the band-limiting filters $g_I(t)$ and $g_Q(t)$ yields different auto-correlation function for QPSK and OQPSK.

Once the complete expression of $R_y(\tau)$ has been derived (this expression is too long to be given in this paper), the PSD $S_y(f)$ of $y(t)$ is obtained by:

$$S_y(f) = \int_{-\infty}^{\infty} R_y(\tau) e^{-j2\pi f\tau} d\tau. \quad (14)$$

4. VALIDATION OF THE ANALYTICAL ANALYSIS

4.1. PA configuration

We consider a nonlinear PA with an AM-AM characteristic described by (3) in which the coefficients a_{2k+1} are real-valued. We normalize both the PA gain a_1 and the PA input amplitude at 1-dB compression point A_{1-dB} to 1. Using the equation (15) from [2], the third-order coefficient a_3 can be calculated as follows:

$$a_3 = -0.145 \frac{a_1}{A_{1dB}^2}. \quad (15)$$

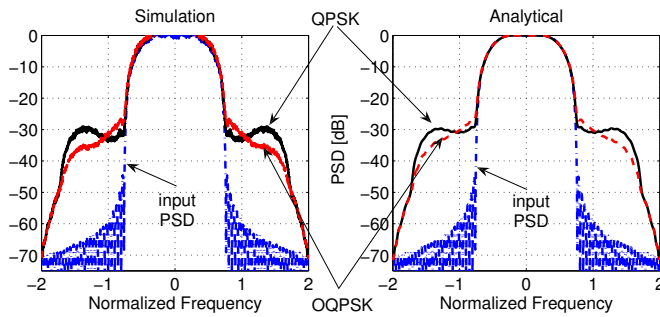


Fig. 2. The PA output PSD obtained from our analytical analysis matches well the simulated PSD for both QPSK and OQPSK.

The parameter a_3 is then equal to -0.145 . The Input BackOff (IBO) is used as a parameter to define the PA operating point relative to A_{1dB} . The IBO has to be kept as low as possible to achieve high power efficiency [2].

4.2. Results

As a first step, we validate the PA output PSD obtained from our analytical analysis by comparing it to the PSD obtained via simulations. Let us focus on two waveforms used by W-CDMA wireless standards based on the QPSK and OQPSK modulation schemes. The transmitted waveform is band-limited using an SRRC filter. Figure 2 shows both the analytical and simulated PSD for an PA IBO of 0 dB and an SRRC filter roll-off equals to 0.3. We observe that the result of our analytical approach matches well the simulation results for both QPSK and OQPSK. Thus, we can predict the PA output PSD using our analytical method without running time-consuming simulations. Next, as shown in Figure 3, we use the obtained analytical PA output PSD to compare the SR of both QPSK and OQPSK as a function of the SRRC roll-off and PA IBO. Therefore, we characterize the SR using the metric Adjacent Channel Power Ratio (ACPR), which is the out-of-band power to the in-band power ratio. We note that for small roll-off, both OQPSK and QPSK have almost the same ACPR. As the roll-off increases, OQPSK experiences less SR relative to QPSK. Furthermore, we observe that by reducing the IBO from 0 dB to -5 dB (i.e. higher power efficiency), the ACPR increases for both QPSK and OQPSK by almost 15 dB. However, the ACPR difference between QPSK and OQPSK remains approximately the same.

5. CONCLUSION

The analytical analysis presented in this paper predicts correctly the PSD of band-limited QPSK and OQPSK signals at the output of a nonlinear PA. Furthermore, using this analytical analysis, we compare the SR of both QPSK and OQPSK as a function of the SRRC roll-off. We conclude that for small

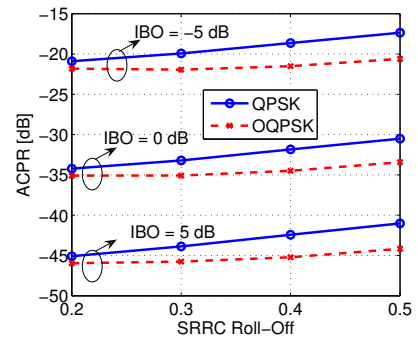


Fig. 3. As the SRRC filter roll-off increases, the ACPR difference between OQPSK and QPSK grows.

roll-off, both QPSK and OQPSK experience almost the same level of spectral regrowth. As the roll-off increases, OQPSK becomes less sensitive to PA nonlinearity relative to QPSK.

6. REFERENCES

- [1] B. Bougard; S. Pollin; G. Lenoir; W. Eberle; L. Van der Perre; F. Catthoor; W. Dehaene, "Energy-scalability enhancement of wireless local area network transceivers," *Signal Processing Advances in Wireless Communications*, pp. 449–453, July 2004.
- [2] B. Razavi, *RF Microelectronics*. Prentice Hall PTR, 1997.
- [3] K. Gard, H. M. Gutierrez and M. B. Steer, "Characterization of spectral regrowth in microwave amplifiers," *IEEE Trans. Microwave Theory Tech.*, vol. 47, July 1999.
- [4] G.T. Zhou and J.S. Kenney, "Predicting spectral regrowth of nonlinear power amplifiers," *Communications, IEEE Transactions on*, vol. 50, pp. 718–722 – 2676, May 2002.
- [5] Raich, R.; Zhou, G.T, "Analyzing spectral regrowth of QPSK and OQPSK signals," *Acoustics, Speech, and Signal Processing, 2001. Proceedings. (ICASSP '01). 2001 IEEE International Conference on*, vol. 4, pp. 2673 – 2676, May 2001.
- [6] S. Benedetto and E. Biglieri, *Principles of Digital Transmission with Wireless Applications*. New York: Kluwer Academic/Plenum Publishers, 1999.
- [7] J.G. Proakis, *Digital Communications*. Mc Graw Hill, 4th ed., 2001.
- [8] J.M Mendel, "Tutorial on higher-order statistics (spectra) in signal processing and system theory: theoretical results and some applications," *Proceedings of the IEEE*, vol. 79, pp. 78 – 305, March 1991.